ERDC TN-SWWRP-07-9
October 2007

Regional Morphology Analysis Package (RMAP): Empirical Orthogonal Function Analysis, Background and Examples

by Kenneth J. Connell and Magnus Larson

PURPOSE: This System-Wide Water Resources Program (SWWRP) technical note describes software for analyzing beach profile and shoreline position data by means of Empirical Orthogonal Functions (EOFs). Patterns obtained through EOF analysis can often be related to the physical processes shaping the beach morphology and extend understanding of how the morphology responds to changes in the forcing (e.g., wave and water level conditions) or to anthropogenic activities (e.g., beach nourishment, coastal structures). EOF analysis capability was added to the Regional Morphology Analysis Package (RMAP). After review of the theory and literature, the EOF method is applied to three examples that encompass (1) beach profiles measured through time at a specific location, (2) beach profiles surveyed at various alongshore locations at a specific time, and (3) shorelines measured at different times.

MOTIVATION: Analysis of morphologic data often constitutes the first step towards understanding the processes shaping the coast. Results from such an analysis may also provide a basis for selecting and applying mathematical models to simulate coastal evolution. The main objective of morphological data analysis is to establish basic properties of the data set and the degree of association between these properties (Larson et al. 2003). Thus, such analysis focuses on detecting and quantifying dominant patterns in the data and their evolution in time and space, as well as how different patterns are related to each other. Empirical orthogonal function (EOF) analysis discussed in this technical note provides a method for determining such basic patterns. The use of a limited set of basic functions to represent the data is often an effective way of distinguishing between signal and noise (Von Storch and Navarra 1995). The signal is associated with the morphological processes at the scale of interest, whereas the noise includes the effects of processes operating at smaller scales not sufficiently resolved by the data, as well as inaccuracies in the measurements. Distinguishing between signal and noise can be difficult and depends on the specific application, as well as on the required accuracy of the data representation.

For long-term data sets such as those extending over decades to centuries, EOF analysis offers an efficient technique to determine characteristic time and space scales of the beach response (De Vriend 1991a; 1991b; Larson and Kraus 1995), as well as to extract general properties of the beach response. The response of a coastal system is associated with changes in the forcing of the system itself, which could be natural, such as shoal evolution at a coastal inlet, or anthropogenic, such as beach nourishment or the construction of a groin or jetty. Another motivation for employing EOF analysis techniques is data reduction where the original data are too extensive to be efficiently managed. Instead, the data are represented through a limited set of functions obtained by using some predefined statistical measure. The functions derived through EOF analysis concentrate the variance of the data in an optimal manner.

EOF analysis is closely related to principal component analysis (PCA). PCA methods have been employed in meteorology and oceanography to resolve the spatial and temporal variability of physical fields (Preisendorfer 1988; Von Storch and Navarra 1995). However, PCA was originally developed by researchers in the field of experimental psychology (Hotelling 1933) and later adopted by geologists (Krumbein and Graybill 1965; Davis 1973). The PCA methods have shown promise in terms of representing complex fields through a limited number of basic patterns (principal components) combined with multiplicative functions (principal component scores). Even though the patterns do not necessarily have physical relevance, it is often possible to give an interpretation that is physically based when beach morphology data are analyzed. This is probably due to the fact that beach morphologies are geometric constructs consisting of different physical features (e.g., dunes, berms, bars, troughs) and the patterns extracted through PCA often match these features. PCA has previously been employed in analysis of coastal data, typically to determine the shape of the EOFs for time series of beach profiles surveyed at a particular location (e.g., Winant et al. 1975; Aubrey 1979), as discussed in the following paragraphs.

BACKGROUND: Eigenvector or eigenfunction techniques encompass the mapping of the observed data onto a set of shape functions (the EOFs) that are extracted from the data set itself (Preisendorfer 1988; Jackson 1991). The term, eigenvector, derives from the German phrase, "own, self, or characteristic" vector as defined by the data. The EOFs correspond to a statistically optimal description of the data with respect to how the variance is concentrated in the modes, where the variance explained decreases monotonically with the mode number. Because the explained variance typically drops at a high rate with the mode number, only a limited number of modes are needed to explain most of the variance. This property is often the motivation for using EOFs as a data reduction technique or a method to separate between signal and noise. Although EOFs are optimal in a statistical sense, there is no a priori reason that the eigenfunctions should have a physical background, even though such interpretations are usually possible, as will be shown through the examples in this technical note.

A data matrix X containing, for example, morphological quantities sampled in space (columns) at specific times (rows), may be represented using matrices involving the principal components E, the eigenvalues, L, and the principal component scores A:

$$X = ELA^T \tag{1}$$

The column vectors in E and A are orthonormal (i.e., vectors are mutually orthogonal and normalized to unit length) and correspond to the eigenmodes, and the variance associated with respective mode is given by the eigenvalue in L. The EOFs (i.e., E and A) are obtained by solving an eigenvalue problem involving the covariance or correlation matrix based on X, but in some applications the sum-of-square matrix is used instead. In the former approach the arithmetical mean is removed, which is the most common method in applications to morphologic data because the mean tends to dominate the signal. Using the sum-of-squares matrix might be more useful in cases where the EOFs are rotated (i.e., are replaced with another pattern to achieve a simpler description according to some criterion) to allow for a more physical interpretation of the eigenvectors (Preisendorfer 1988; Von Storch and Navarra 1995).

The number of modes (and associated eigenvalues) obtained from an EOF analysis equals the lowest value with respect to the number of rows M and columns N in the data matrix, that is, for a matrix of dimension $M \times N$ the number of modes is the smallest value of M and N. If $M < N$, the matrix E will have the dimensions $M \times M$ and the matrix A the dimensions $M \times N$. In solving the eigenvalue problem to obtain the eigenvector modes, it is sometimes convenient to transpose the data matrix to arrive at a covariance or correlation matrix with the smallest possible dimensions (equal to the number of modes). Such an operation may often speed up the computations significantly. Thus, if $M > N$, the data matrix is transposed to yield an $N \times M$ matrix with N eigenvector modes. Traditionally, when EOF analysis of beach profiles measured at a specific location through time has been performed, the principal components have yielded the cross-shore patterns (often denoted as spatial EOFs), and the principal scores are the time functions (temporal EOFs). However, if the data matrix is transposed, the opposite may occur, that is, the principal components yield the variation in time and the scores the variation in space. This is just a matter of convenience and does not affect the actual results of the EOF analysis.

A disadvantage of traditional EOF analysis is the inability to resolve fixed patterns in the data that propagate with time. Thus, progressive wave-like motions are represented as combinations of standing waves and the characteristics of propagating patterns cannot be quantified by the technique (e.g., wave speed and wavelength). However, modifications of the EOF analysis have been developed to remedy this deficiency, namely extended EOF analysis (EEOF) and complex PCA (CPCA). In EEOF analysis, the original data set is extended by adding lagged observations in time after which traditional EOF analysis is performed (Weare and Nasstrom 1982). A disadvantage of the EEOF is that the approach becomes computer-intensive as the number of time lags increases. In CPCA, a new data set is formed from the original set and its Hilbert transform (Horel 1984). Then, complex eigenvectors are determined by applying EOF analysis to the derived complex data set. CPCA has a good potential for identifying traveling patterns in the data, although the interpretation is more difficult than EOF analysis because both amplitude and phase relationships must be considered. Further, CPCA, or any modification of the EOF technique involving time-lagged data, requires the data to be sampled with a constant time interval, which is often not the case for coastal morphology data.

PREVIOUS APPLICATIONS OF EOF ANALYSIS IN COASTAL MORPHOLOGY: EOF analysis was originally applied in coastal morphology in the middle of the 1970s to investigate variations in the beach profile shape in space and time (Hayden et al. 1975; Winant et al. 1975). These studies showed that distinct morphologic characteristics could be associated with the lower EOF modes. For example, Aubrey (1979) related the mean profile shape, bar and berm features, and the low-tide terrace to the first, second, and third EOF modes, respectively (the mean was not subtracted in the analysis). After these pioneering studies, EOF analysis became a fairly commonly applied technique in investigating beach profile response over time scales of several years. Larson and Kraus (1994) employed this technique to investigate the alongshore uniformity of profile response and to determine characteristic shapes of the longshore bars at Duck, NC. Rozynski (2003) used EOF analysis to determine the characteristic evolution patterns of multiple longshore bars at a beach on the Polish coast in the southern part of the Baltic Sea.

Larson et al. (1999) analyzed complete bottom topographies by EOF's at three different locations in the United States with the aim of separating between different types of forcing and the signals that arose from the data. The study sites were locations of beach nourishment operations during

the period when the data were collected. The EOF analysis performed identified signals from severe storms, effects of complex bottom topographies (e.g., shore-attached shoals), and the placement of the nourishment. Haxel and Holman (2004) studied the bottom topography from surveyed data at Agate Beach, OR, using eigenfunctions. Two distinct eigenmodes were resolved in the data associated with seasonal patterns of sediment flux, where the first mode was related to the summer growth of a dune field, and the second mode associated with the changes in the beach due to waves.

More advanced eigenvector techniques have also been applied to beach topography data in some cases, for example CPCA (Liang and Seymour 1991; Liang et al. 1992) and three-mode PCA (Medina et al. 1992). Yokoki and Larson (2004) employed CPCA to analyze the topographic evolution at the Island of Sylt, Germany, with the attempt to establish the properties of rhythmic features in the alongshore direction. To identify the dominant modes for the topographic change at any given point, a local ratio of contribution was defined. In traditional CPCA averaged values over the whole region are obtained in the analysis, and no detailed information at a particular location is provided (see also Kroon et al. in preparation). Ruessink et al. (2004) employed nonlinear CPCA to extract propagating spatial patterns that constituted the most dominant components in three data sets encompassing measured profiles surveyed at Egmond, The Netherlands; Duck, NC; and Hasaki Beach, Japan. For the Egmond and Hasaki data sets, the nonlinear CPCA provided a more complete description of the data than the standard CPCA, if the lower modes were considered. However, for the Duck data, where the amplitude changes of the nearshore bars were larger, applying nonlinear CPCA did not improve characterization of the data.

For revealing patterns in data sets on nearshore topography that are spatially extensive but temporally sparse, a combination of the EOF technique with a moving window approach can prove useful (Wijnberg 1995; Wijnberg and Terwindt 1995). EOFs may also be incorporated with numerical modeling if the associated time functions can be predicted over the simulation period. Aubrey et al. (1980) tried to predict daily and weekly beach changes over a 5-year period from offshore wave properties using linear statistical predictor techniques to obtain A (see also Hsu et al. 1986 and Hsu et al. 1994).

EXAMPLE APPLICATIONS OF EOF ANALYSIS TO BEACH PROFILES AND SHORELINES: The EOF analysis may be applied to either beach profiles or shorelines measured in time or to beach profiles measured at a number of alongshore locations (i.e., a beach topography survey). In principle, time sequences of measured topographies can also be analyzed, if all profile lines surveyed at a specific time are concatenated (i.e., placed after each other) and entered as column vectors in the data matrix. The analysis of topographies typically requires some additional data manipulation including interpolation as well as concatenating and splitting up data matrices after the analysis. The examples discussed in the following cover 1) beach profiles surveyed in time at a specific location, 2) beach profiles surveyed at a number of alongshore locations at a specific time, and 3) shorelines measured in time. In order to interpret the EOF modes, the eigenvectors and principal scores should be considered simultaneously because they are entered as a product in Equation 1. All calculations and plots were done with RMAP.

Beach profiles in time. An investigation of beach profiles (Stauble et al. 1993) along Fenwick Island in the vicinity of Ocean City, MD (Figure 1) provides a good basis for an application of EOF analysis. The beach profile data set examined in this study ranges from the north jetty at Ocean City Inlet at the southern extent (Transect OC1) to the beach adjacent to Little Assawoman Bay at the northern extent near the Delaware state border (Transect OC46). The profiles were surveyed at approximately 500 m interval alongshore. Although the profiles were not surveyed at equal intervals in time, the data set covers a temporal range of 10 years (1995-2005) with the profile lines surveyed once or twice per year.

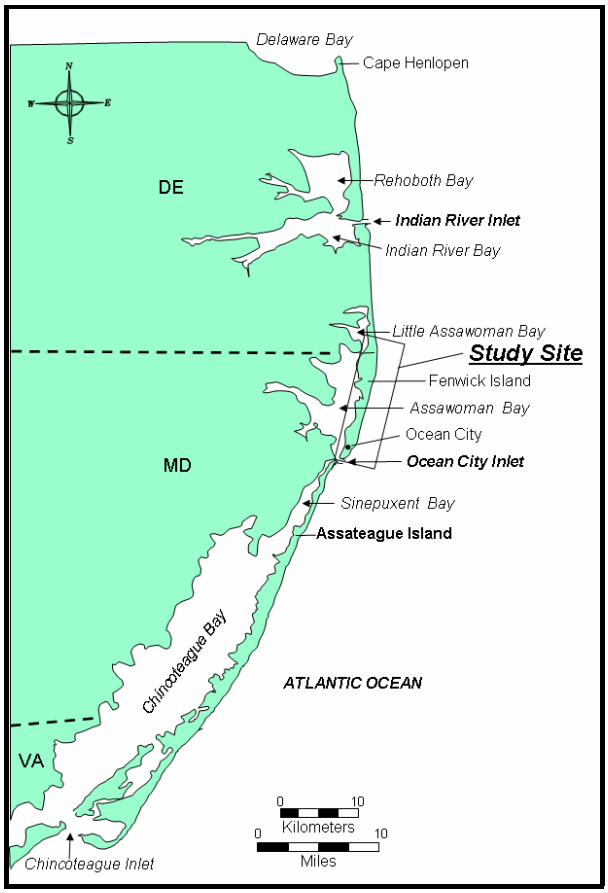

Figure 1. Location map with study extents shown in the box.

First, a temporal eigenfunction analysis was conducted for all profiles taken at each transect. Transect OC13 (37th Street beach profile) is provided as the example for discussion in this technical note because of its relative distance from the local morphologic influence of Ocean City Inlet and for its complete data coverage of the sampling intervals. The first three eigenvalues account for 93 percent of the total variance at 72, 18, and 3 percent, respectively for OC13 (mean removed, as was done in all the analyses discussed here). Figure 2 shows the relative weighting of all the eigenvalues, and it can be assumed that mode 6 and greater are noise, whereas modes 3, 4, and 5 have large contributions from noise in the signal.

The sparse and irregular sampling interval of the temporal data set makes it difficult to extract a clear seasonal signal in the EOF analysis. However, inspection of the first principal score (Figure 3, red) reveals a relationship to bar erosion and accretion. Profiles surveyed in 1996 showed significant erosion after a stormy period during winter 1995/1996 (Stauble and Bass 1999), and negative variation in the first principal score shows this signal in the middle of 1996. A beach fill was placed during spring and fall of 1998 (Stauble and Bass 1999), which supplied more sediment to the bar in subsequent years as shown by the positive variation in the first principal score starting at the end of 1998. The second principal score (Figure 3, blue) may correspond directly to beach berm erosion and accretion. Negative values of the second principal score mode correspond with berm erosion associated with stormy periods (waves > 3m in Figure 4) during 1996, 1999, 2003, and winter 2003/2004. It should be noted that the 1998 beach profile was a post-fill profile and does not reflect erosion from the winter storms associated with the 1997/1998 El Niño.

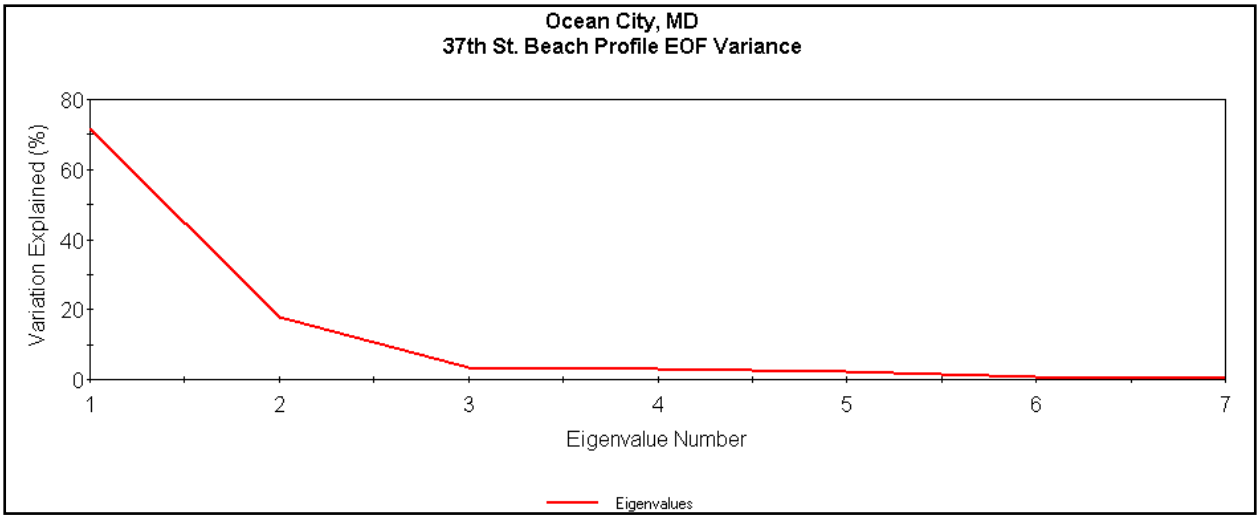

Figure 2. Eigenvalue variance for profiles in transect OC13 (37th St).

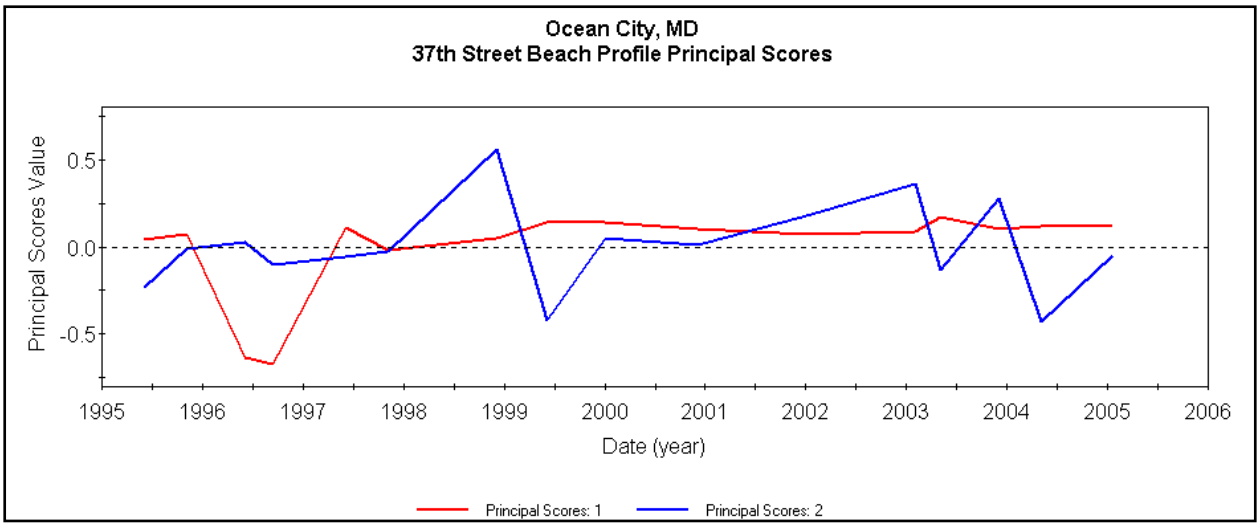

Figure 3. First two modes of the principal scores (temporal patterns) from the temporal analysis of transect OC13.

Further investigation into the period that follows the completion of the fall 1998 beach fill leads to analysis of the profiles that bookend the greatest variation in the second principal score (Figure 3, blue) between 1998 and 1999. Figure 5 presents the profiles before beach renourishment (October 1997, green), post-fill (November 1998, red), and after equilibration (May 1999, blue) along with the first two modes of the cross-shore eigenvectors superposed over the profiles. It is evident that a large volume of sediment from the berm and foreshore from the November 1998 profile (Figure 5, red) moved into the offshore bar at some point before the May 1999 (Figure 5, blue) profile. In this case, the first eigenvector mode (Figure 5, black) follows the profile envelope (Figure 6, red = maximum envelope, blue minimum envelope) and is similar to the standard deviation (Figure 6, black). The first cross-shore mode in this example can be used to quickly examine regions of greatest change along the complete set of profiles. The second eigenvector mode (Figure 5, magenta) may be interpreted to represent bar-berm movement. This example (Figure 5) shows the maximum at the post-fill (Nov. 1998) berm, and a minimum at the bar that develops in the May 1999 profile after profile equilibration.

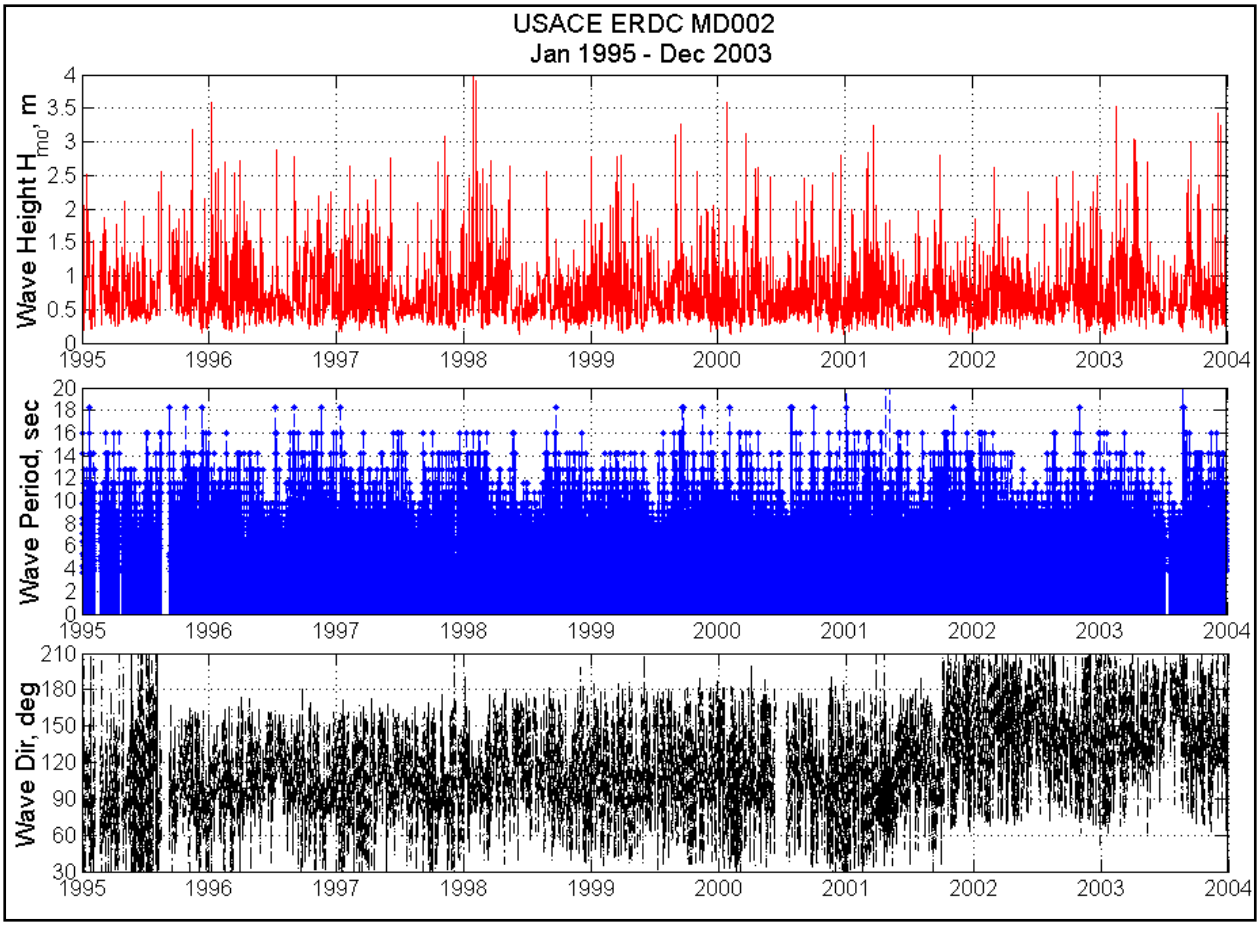

Figure 4. Wave height, wave period, wind direction, and wind speed at USACE ERDC wave gauge MD002 for 1995-2004.

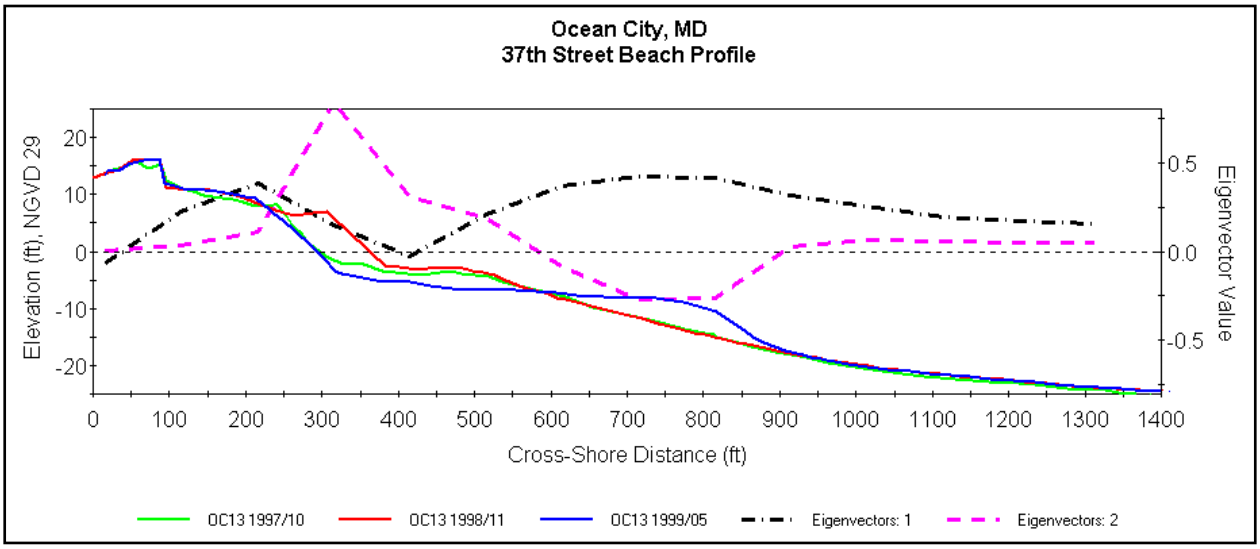

Figure 5. October 1997, November 1998, and May 1999 profiles and first three eigenvector modes (cross-shore patterns) at OC13 (37th Street Profile).

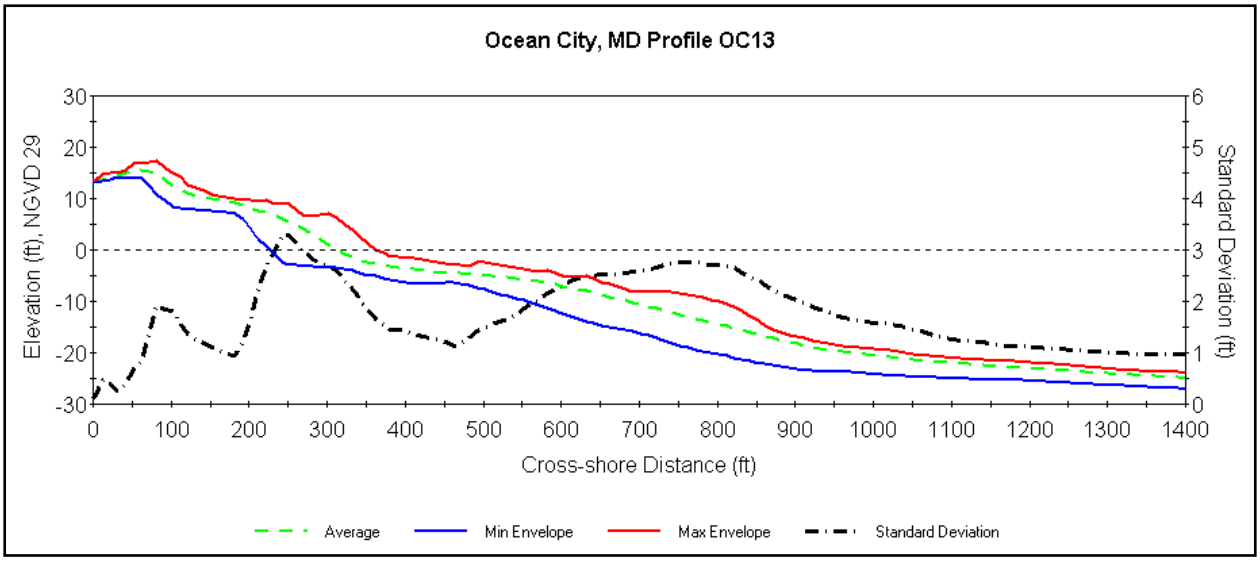

Figure 6. October 1997, November 1998, and May 1999 profile envelope and standard deviation at OC13 (37th Street Profile).

The two event signals correspond to profile readjustment after a series of storms in the area. Figure 7 is a time series of offshore significant wave height from a wave gauge maintained by the U.S. Army Corps of Engineers (USACE), Engineer Research and Development Center (ERDC) station MD002 offshore of Ocean City for the period between 1 Oct 1997 and 31 May 1999. A beach-fill project commenced in 1998 following a period of severe storms during the winter 1997/1998 El Niño (Stauble and Bass 1999). The 1998 post-fill profile (Figure 5, red) was surveyed in Nov 1998 during a relatively calm period, and shows the large area of accretion on the berm due to the beach fill. Moderate storms in January and March 1999 (Figure 7), prior to the May profile survey (Figure 5, blue), likely generated waves that moved a large volume of sand from the beach berm to the offshore bar.

Beach profiles in space. A spatial two-dimensional (2-D) eigenfunction analysis was also conducted to examine alongshore variation in the profiles within the study site (Figure 1). Initially, the spatial eigenfunction analysis was conducted on all available transects (OC1 – OC46). However, the presence of the large updrift fillet adjacent to the north jetty of Ocean City Inlet appeared in profiles OC1-OC8 as a significant cross-shore mass of sand that steadily decreased in each profile north and dominated the alongshore spatial signal so that any spatial variation in profiles north of the fillet appeared as noise. Therefore, the spatial EOF was applied to those transects north of the primary influence of the Ocean City Inlet fillet (OC9 – OC46) with an assigned cross-shore sampling interval of 15 ft, and an alongshore sampling interval of 2,000 ft. The spatial analysis was conducted for the profiles surveyed in April 2004 and the profiles surveyed in June 2005. Again, 90 percent of the variance is explained in the first three modes of both the 2004 and 2005 analysis (Figure 8). In this spatial EOF analysis, the first mode explains 70 percent of the variance for April 2004 and 75 percent of the variance for June 2005 and the second mode explains 15 percent of the variance for April 2004 and 13 percent of the variance for June 2005.

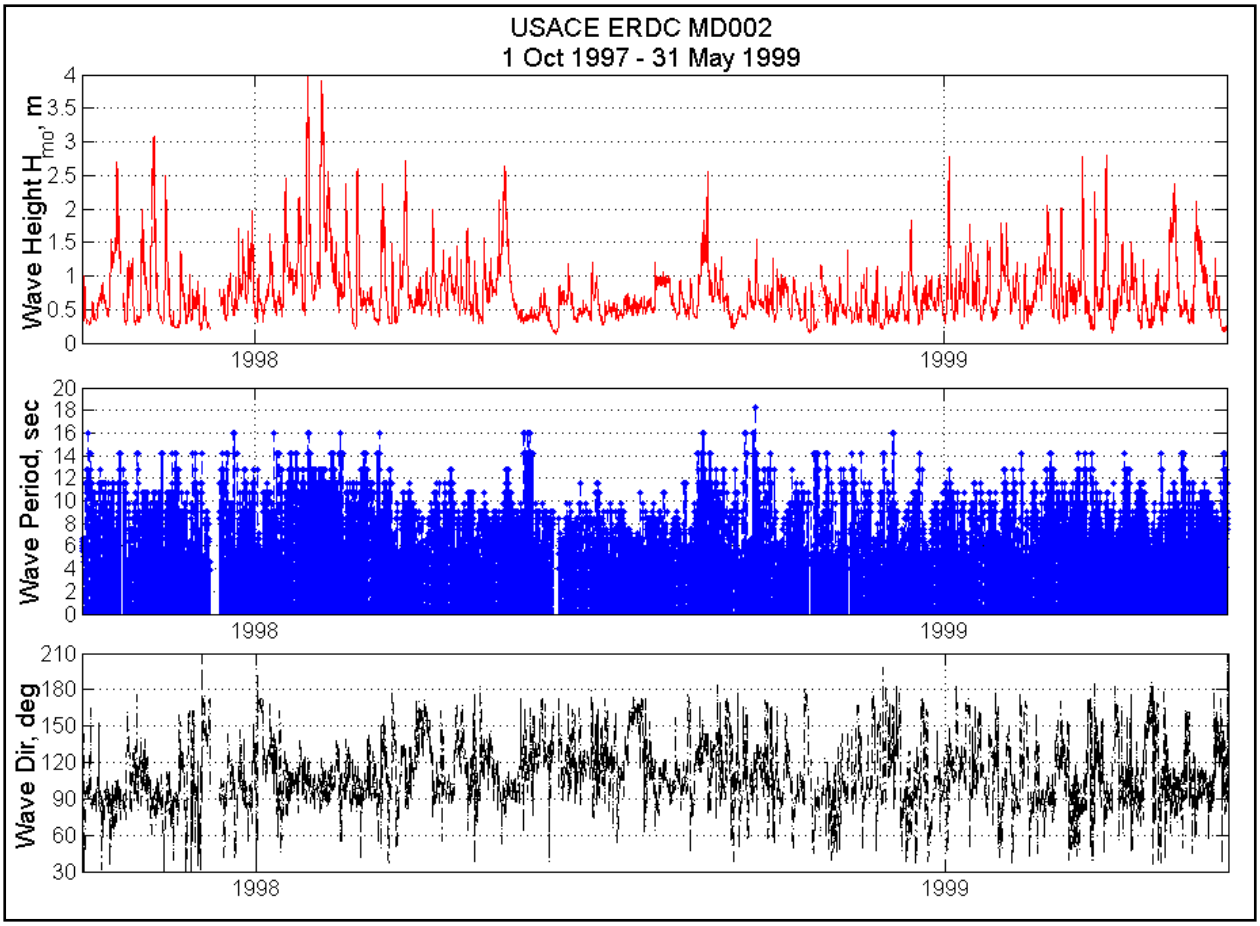

Figure 7. Wave height, wave period, wind direction, and wind speed at NDBC bouy 44009 for first six months of 1999.

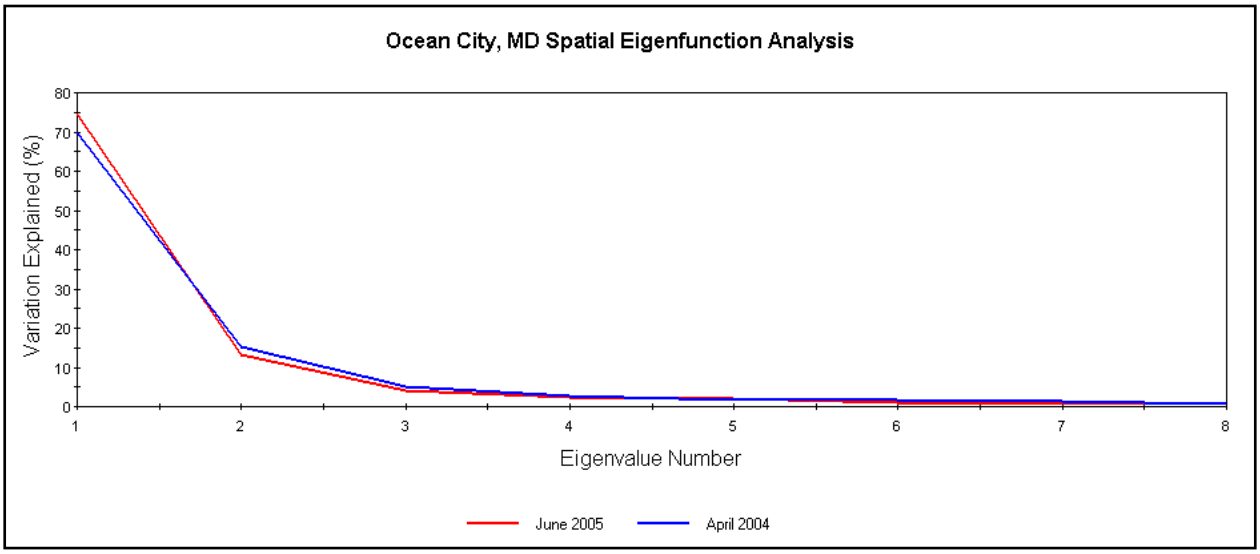

Figure 8. Eigenvalue variance for profiles for April 2004 (blue) and June 2005 (red) spatial EOF analysis.

The first three modes of this EOF analysis (Figures 9 and 10; cross-shore patterns) show a different signal. The first mode (Figures 9 and 10, red) appears to show the relative differences across the profiles, much of this relative difference may be explained by beach fill response and storm response. This mode has maxima at the beach berm/foreshore and at the offshore bar. The second mode (Figures 9 and 10, black) represents the beach-face signal with a single maximum in the vicinity of the beach face and a minimum at the bar. Finally, the third mode (Figures 9 and 10, blue) could be interpreted to represent topographic slope breaks with high positive amplitude at the offshore terrace just before the profile slope steepens, but signal noise contributions and the three dimensional nature of the alongshore profile variations make the third mode difficult to interpret.

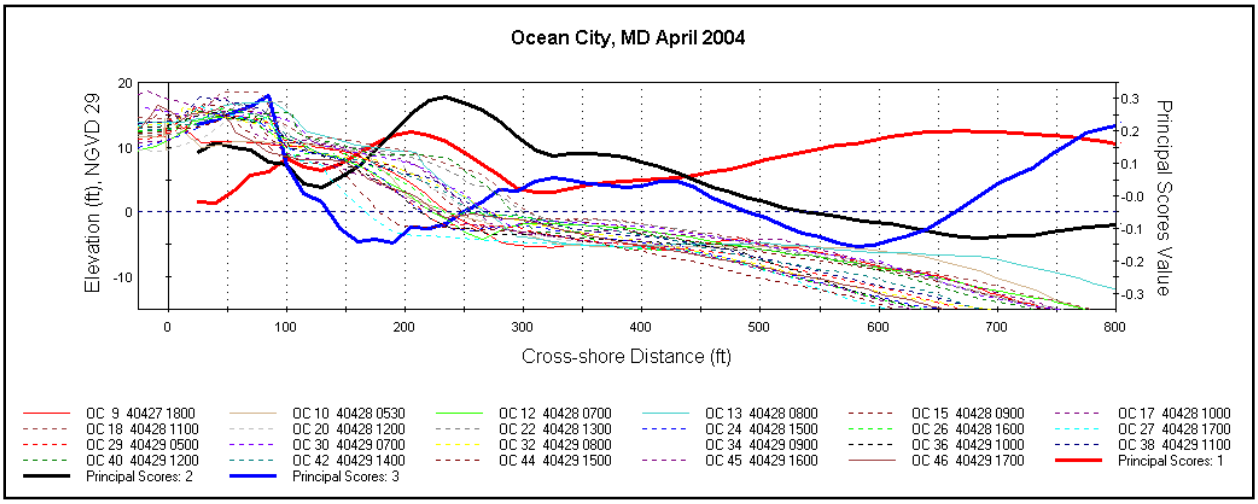

Figure 9. First three principal scores (cross-shore patterns) superimposed over the profiles at sampled transects for April 2004.

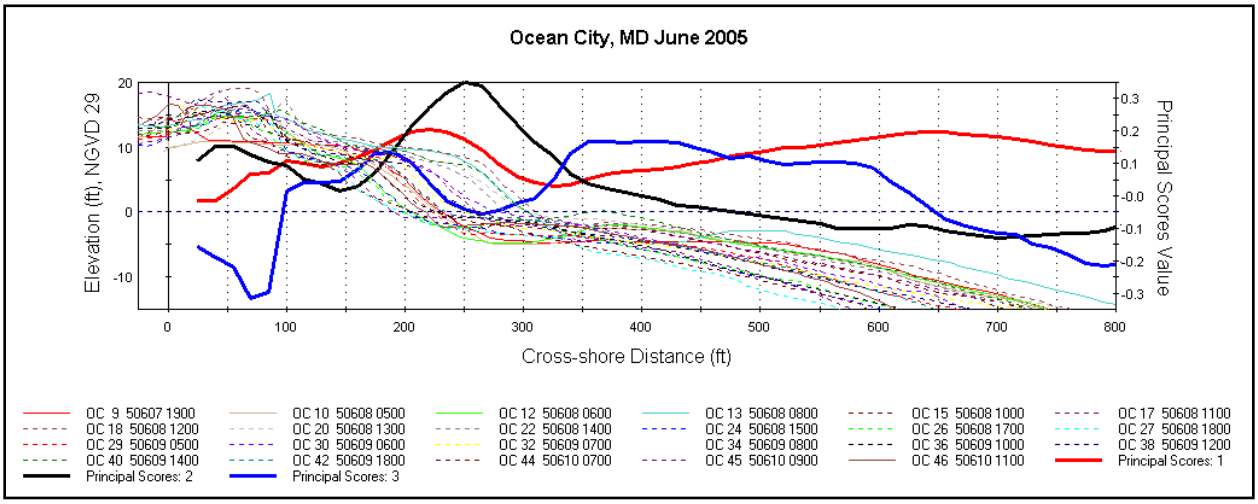

Figure 10. First three principal scores (cross-shore patterns) superimposed over the profiles at sampled transects for June 2005.

Shorelines in time. EOF analysis was also conducted on approximately 100 km of Maryland shoreline to search for signals in shoreline change over time. First, the shoreline change between 1943 and 2002 was examined based on measurements to find regions along the coast with large magnitude of change. The method for conducting shoreline change analysis in RMAP is

discussed in the RMAP user's guide and tutorial (Batten and Kraus 2005). Figure 11 shows large rates of shoreline recession at Assateague Island directly south of Ocean City Inlet and accretion updrift (north) of Ocean City Inlet.

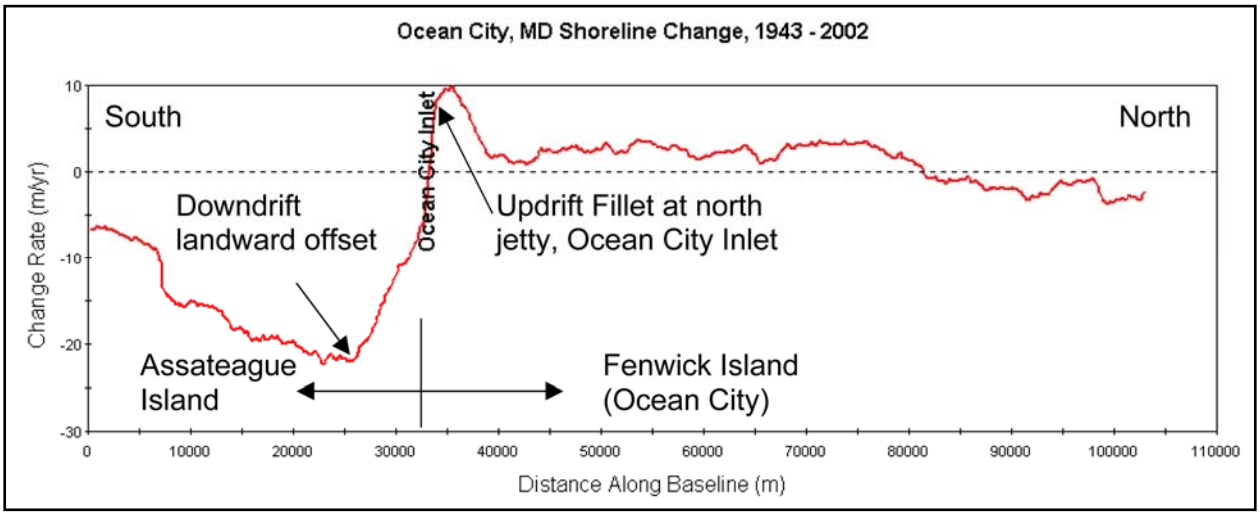

Figure 11. Shoreline change around Ocean City Inlet between 1943 and 2002.

The first two modes of the principal scores (alongshore pattern) in the EOF analysis (Figure 12) also display this large change in shoreline position around the inlet. The EOF analysis was conducted on four shoreline data sets (1943, 1962, 1980, and 2002) derived from aerial photographs and topographic surveys. The first principal score represents the shoreline change signal well with high positive amplitude in regions of recession and high negative amplitude in regions of shoreline growth. The location of Ocean City Inlet is also clearly evident in the first two principal scores, marked by a large magnitude change in amplitude from positive to negative over a short alongshore distance.

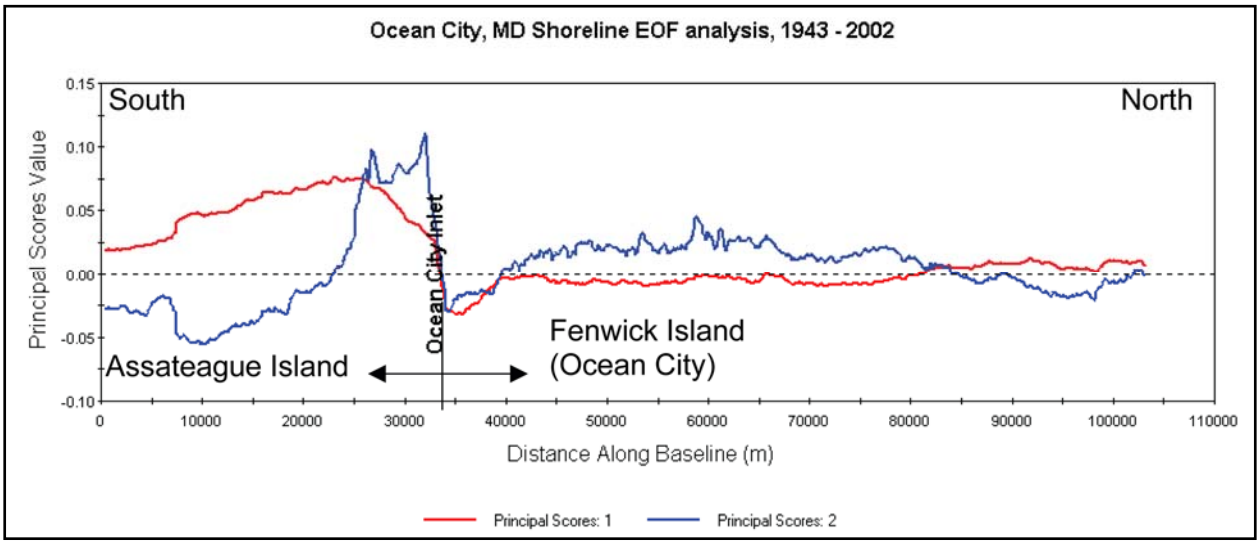

Figure 12. First two modes of the principal scores (alongshore pattern) from EOF analysis on shorelines measured 1943, 1962,1980, and 2002.

RMAP USER'S GUIDE FOR EOF ANALYSIS: This study was conducted as a series of tests of the newly implemented 2-D empirical orthogonal function analysis module in RMAP. The module is accessed and controlled through a tool button ("EOF") that has been added to the analysis toolbar in RMAP (Figure 13).

Figure 13. RMAP toolbar with the EOF analysis tool button (labeled EOF in red).

The goal of the addition of EOF capability in RMAP is to provide a relatively simple, efficient, and practical method of conducting 2-D eigenfunction analysis for practicing engineers and scientists. The addition of EOF capability to RMAP creates a powerful EOF tool for analyzing and visualizing results for large quantities of beach profile and shoreline data, such as occur in regional studies.

To conduct the analysis, one must first import the beach profile or shoreline survey data upon which the analysis is to be conducted. The data import and analysis methods are described in the RMAP user's guide and tutorial (Batten and Kraus 2005). Care should be taken to ensure that the dates of profiles or shorelines are correct in the date region of the metadata window in the lower-right portion of the interface. All time intervals are calculated from the dates provided in this field.

Once the data are imported, the user should select the profiles or shorelines to be included in the analysis, and then click the  button on the analysis toolbar. This action opens the eigenfunction analysis window (Figure 14). The eigenfunction analysis window is where the user selects whether a spatial analysis (i.e., a series of beach profiles surveyed at approximately the same time over a given longshore distance) or a temporal analysis (i.e., a series of profiles or shorelines surveyed in approximately the same location over a given time interval) is to be conducted on the data.

In the case where EOF analysis is executed on shorelines, only temporal analysis (i.e., shoreline change over time) is possible. For shorelines, the eigenfunction analysis domain window does not appear after the EOF analysis  button is pressed. Instead, the shoreline sampling interval window (Figure 15) appears. This is where the user selects the alongshore sampling interval for the EOF analysis, which assigns the resolution of the shorelines. When the user selects *OK* on this window, the baseline selection window for shoreline analysis (Figure 16) appears. Here the user must select the baseline alignment to conduct the shoreline EOF analysis upon. The option of selecting a baseline landward or seaward of the

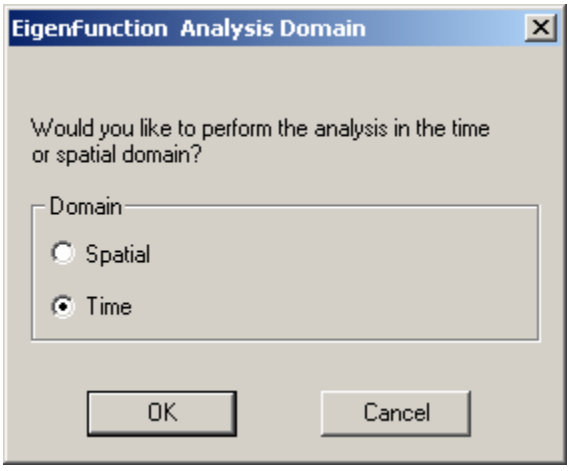

Figure 14. Eigenfunction analysis domain window.

shoreline is also given here. The baseline must be defined as a reference distance to convert the X- and Y-coordinates to an alongshore distance (reference distance along the baseline) and cross-shore distance (offset referenced from the baseline), respectively. The procedure for defining a baseline in RMAP is outlined in Batten and Kraus (2005).

If the user is interested in performing a temporal analysis on beach profiles, the *time* radio button should be selected in the eigenfunction analysis domain window (Figure 14) and the user must then click *OK*. At this point, the eigenfunction analysis temporal domain window (Figure 17) appears. The user enters in the cross-shore starting (*XOn*) and ending (*XOff*) distances and the sampling interval (*Dx*). Defaults are given as the greatest common denominator that has an overlap point of all the profiles in the analysis.

If the user is interested in performing a spatial analysis on beach profiles, the *spatial* radio button should be selected in the eigenfunction analysis domain window (Figure 14) and the user must then click *OK*. At this point, the eigenfunction analysis spatial domain window (Figure 18) appears. The user enters the cross-shore starting (*XOn*) and ending (*XOff*) distances and the cross-shore sampling interval (*Dx*) and the alongshore sampling interval (*Dy*). Again, defaults are given as the greatest common denominators that have an overlap point of all the profiles in the analysis.

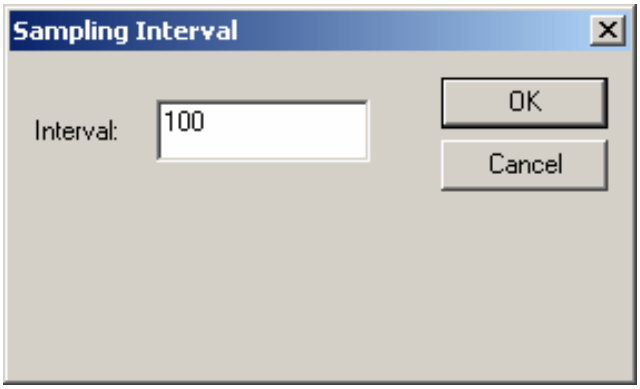

Figure 15. Shoreline sampling interval window.

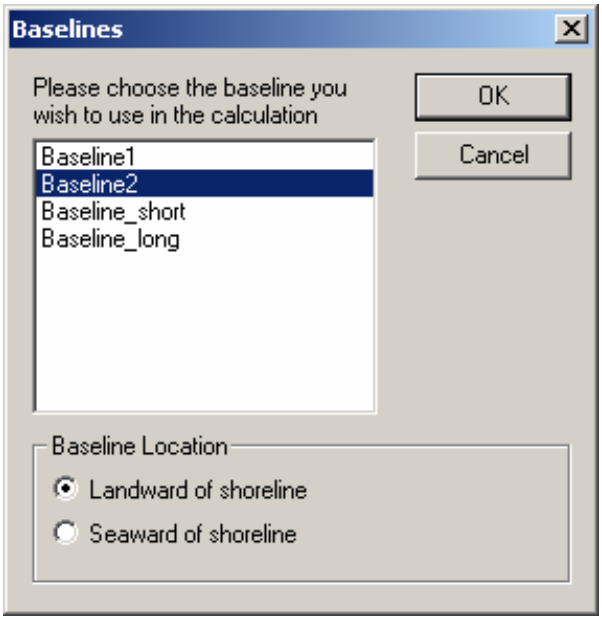

Figure 16. Baseline selection window for shoreline EOF anaylsis.

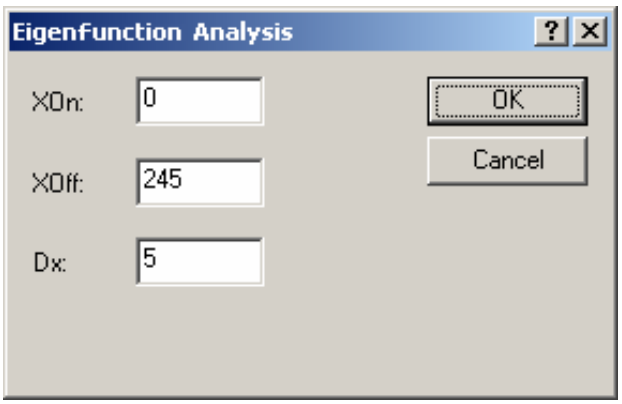

Figure 17. Eigenfunction analysis temporal domain window.

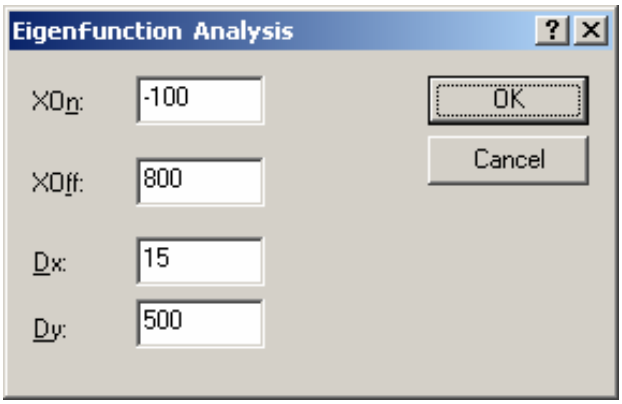

Figure 18. Eigenfunction analysis spatial domain window.

Finally, when the user selects *OK*, RMAP conducts the EOF analysis and generates the output files. The resulting output files appear in the data tree (Figure 19) and consist of the eigenvalues, eigenvectors, principal scores, and an approximation of the input profiles using a limited number of modes.

When the *eigenvalues* file is selected in the data tree (Figure 19), the table of the eigenvalues and their respective variance and explained variance of the total variance appears in the data table (Figure 20) in the lower portion of the RMAP interface.

These values are also graphically represented in the eigenvalues plot (Figure 21) in the main RMAP interface window.

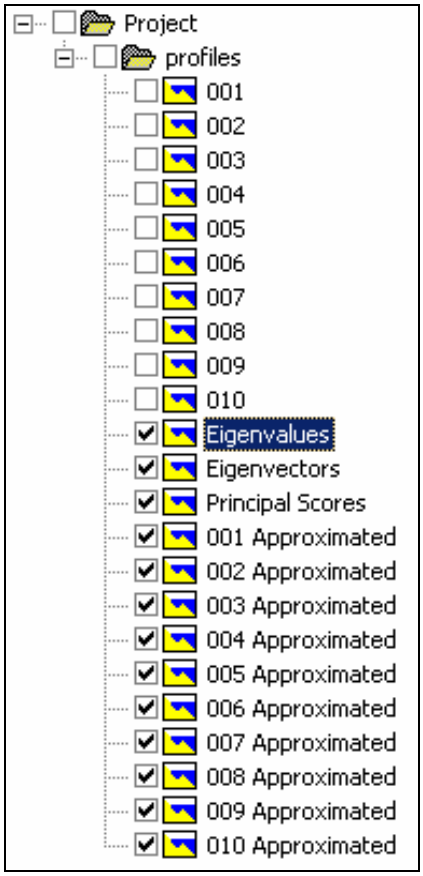

Figure 19. EOF output resulting files in data tree.

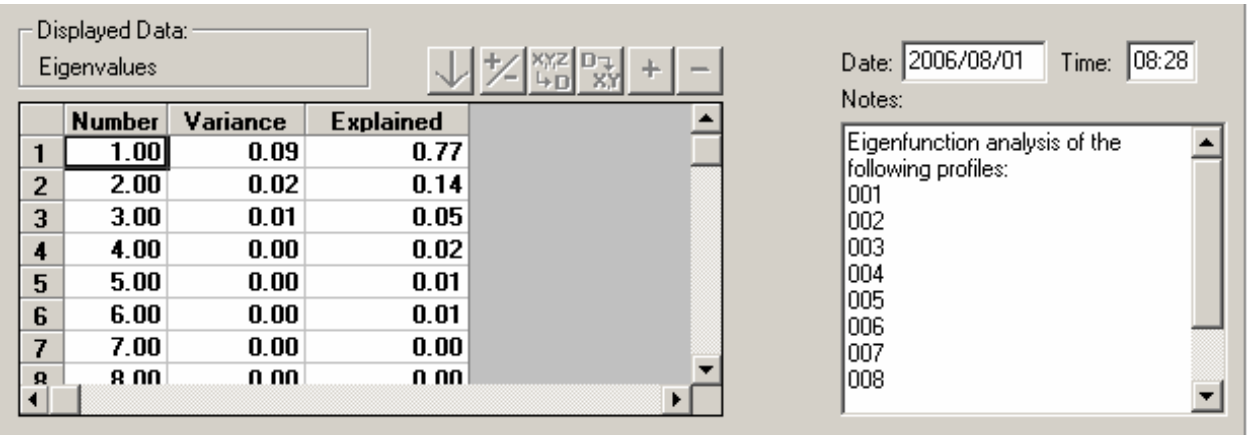

	Number	Variance	Explained
1	1.00	0.09	0.77
2	2.00	0.02	0.14
3	3.00	0.01	0.05
4	4.00	0.00	0.02
5	5.00	0.00	0.01
6	6.00	0.00	0.01
7	7.00	0.00	0.00
8	8.00	0.00	0.00

Figure 20. Eigenvalue table.

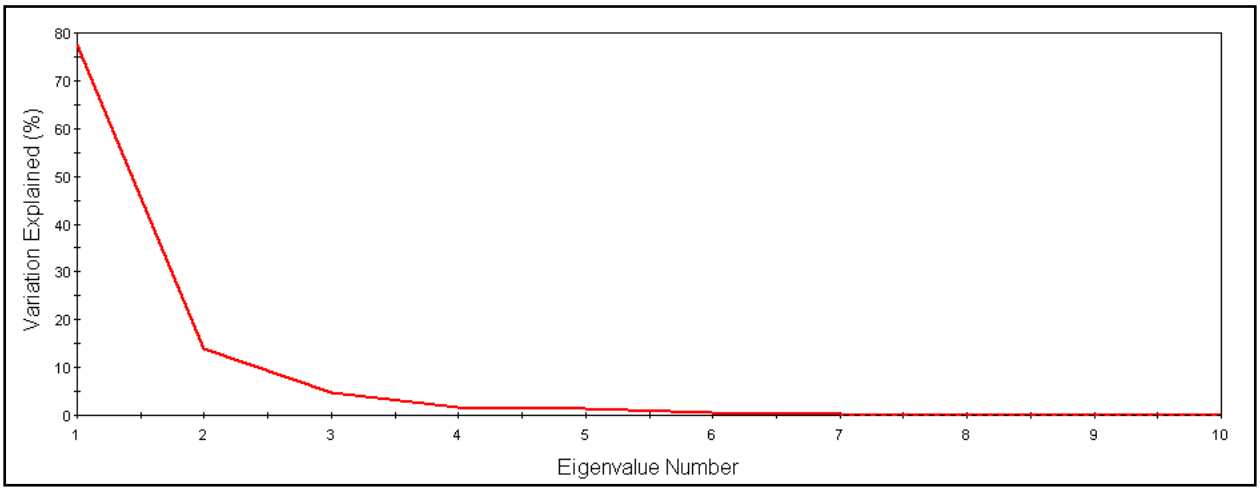

Figure 21. Eigenvalues plot.

When the *eigenvectors* file is selected in the data tree (Figure 19), the data table (Figure 22) shows each column of the eigenvector modes for every cross-shore distance row (for the temporal analysis; Figure 22 a.) and time in days (for the spatial analysis; Figure 22 b.). The boxes in the first row of the data table (Figure 22) may be checked or unchecked to turn the plots of each eigenvector (Figure 23) on or off. This is useful for displaying only the eigenvectors with the greatest explained variance while ignoring the eigenvectors that are primarily attributed to noise in the signal.

The plot of the resulting eigenvectors (Figure 23) may be optimized for visualization in the same way as for beach profiles (Batten and Kraus 2005). Likewise, the eigenvectors may be superimposed upon the profiles or shorelines for comparative analysis. The example provided in this analysis (Figures 22-26) is from a sensitivity test on the EOF module and is a subset of the Duck, NC EOF analysis performed by Larson and Kraus (1994) to examine the capabilities of the RMAP EOF module.

a.

Displayed Data:
Eigenvectors

Date: 2006/08/01 Time: 08:28
Notes:
Eigenfunction analysis of the following profiles:
001
002
003
004
005
006
007
008

	Dist	Vector 1	Vector 2	Vector 3	Vector 4	Vector
1						
2	0.00	0.37	-0.23	-0.69	-0.07	-0.34
3	5.00	0.40	0.11	0.00	0.07	0.08
4	10.00	0.34	0.10	0.38	0.50	0.05
5	15.00	0.40	0.17	0.11	-0.24	0.27
6	20.00	-0.03	-0.54	0.49	-0.47	-0.04
7	25.00	-0.30	-0.45	0.01	0.22	-0.17
8	30.00	-0.32	-0.11	-0.35	-0.01	0.75

b.

Displayed Data:
Eigenvectors

Date: 2006/08/01 Time: 08:57
Notes:
Eigenfunction analysis of the following profiles
001
002
003
004
005
006
007
008

	Time	Vect	Vect	Vector	Vector 4	Vector 5	Vecto
1							
2	0.00	-0.04	-0.09	0.10	-0.22	0.03	0.
3	200.00	-0.04	-0.09	0.22	-0.11	-0.17	-0.
4	400.00	-0.08	-0.18	0.27	0.15	-0.39	-0.
5	600.00	-0.16	-0.35	0.33	0.16	-0.35	0.
6	800.00	-0.13	-0.40	0.24	0.20	-0.06	0.
7	1000.00	0.05	-0.34	0.12	0.16	0.23	-0.
8	1200.00	0.21	-0.23	0.17	0.16	0.32	-0

Figure 22. Eigenvectors table from temporal analysis (a) and spatial analysis (b).

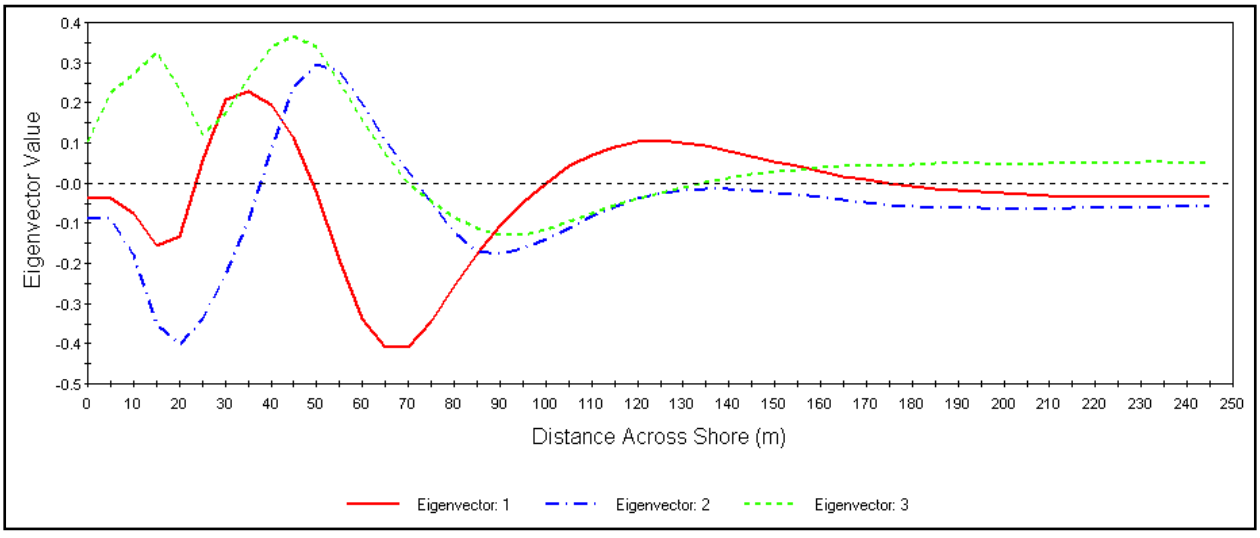

Figure 23. Plot of the first three eigenvectors (cross-shore patterns) from a temporal sensitivity analysis on data collected at Duck, NC.

When the *principal scores* file is selected in the data tree (Figure 19), the data table (Figure 24) shows each column of the principal score modes for each time interval in days (for the temporal analysis) and for each cross-shore distance row (for the spatial analysis). Similar to the

eigenvectors, the boxes in the first row of the data table (Figure 24) may be checked or unchecked to turn the plots of each principal score (Figure 25) on or off.

Figure 25 illustrates an example of the principal scores (temporal patterns) for two years from the temporal analysis conducted on the Duck, NC beach profile subset.

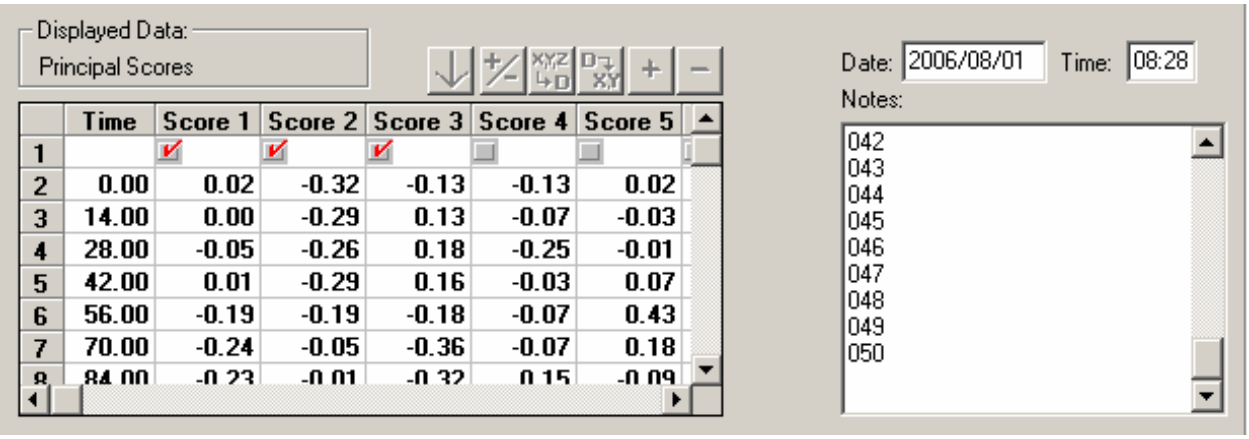

	Time	Score 1	Score 2	Score 3	Score 4	Score 5
1		☑	☑	☑	☐	☐
2	0.00	0.02	-0.32	-0.13	-0.13	0.02
3	14.00	0.00	-0.29	0.13	-0.07	-0.03
4	28.00	-0.05	-0.26	0.18	-0.25	-0.01
5	42.00	0.01	-0.29	0.16	-0.03	0.07
6	56.00	-0.19	-0.19	-0.18	-0.07	0.43
7	70.00	-0.24	-0.05	-0.36	-0.07	0.18
8	84.00	-0.23	-0.01	-0.32	0.15	-0.09

Figure 24. Principal scores table.

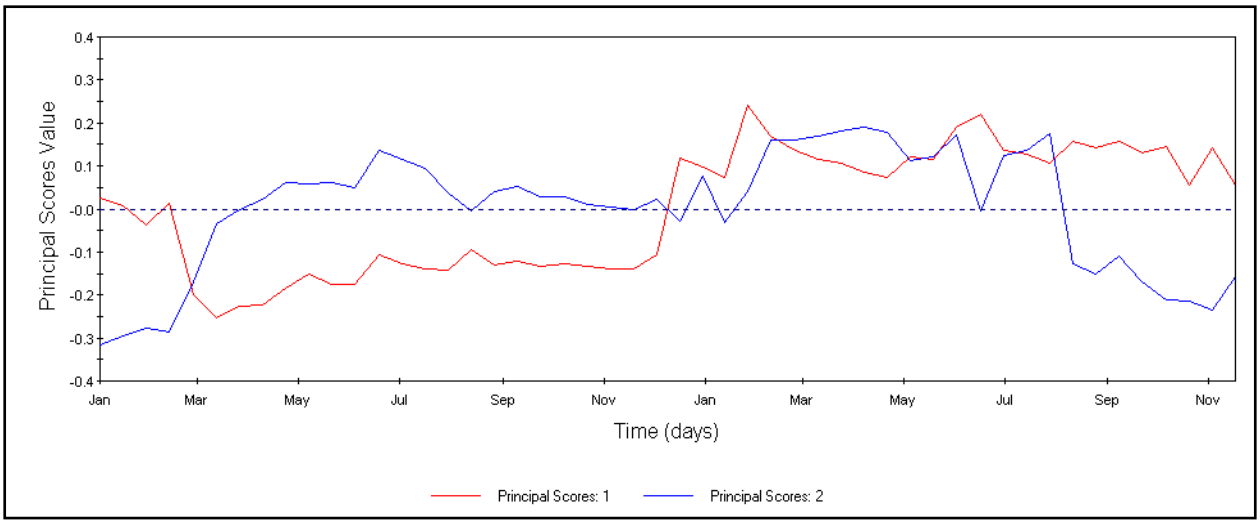

Figure 25. Plot of the first two principal scores (temporal patterns) from a temporal sensitivity analysis on data collected at Duck, NC.

The first mode of the principal score in this case depicts the contrast between gently sloping profiles and profiles with more developed bars and troughs. The second mode of the principal score in this case detects the temporal bar-berm migration signal fairly well. Points of increased variability in the second mode (Figure 25) were selected as the basis for averaging periods in Figure 26. The average profiles (Figure 26) that match the amplitude changes in the second mode of the principal score (Figure 25) indicate seasonal movement of the bar. This is not a perfect seasonal signal as there is some seasonal variation associated with wave energy differences from year to year. However, one can clearly detect the shallow bar and deep trough associated with the negative values of the second principal score in the January through February time period. As the

second mode of the temporal function moves to a low positive value between March and December, the average bar elevation decreases and levels as it extends offshore and the foreshore increases in width. An increase to a high positive value of the second principal score between January and July may be associated with the deepening of the offshore plateau and buildup of the nearshore bar. As the second mode of the temporal function returns to a negative value, the average profile associated with the August through November time period returns to a shallow bar and deep trough configuration similar to the initial January through February average profile.

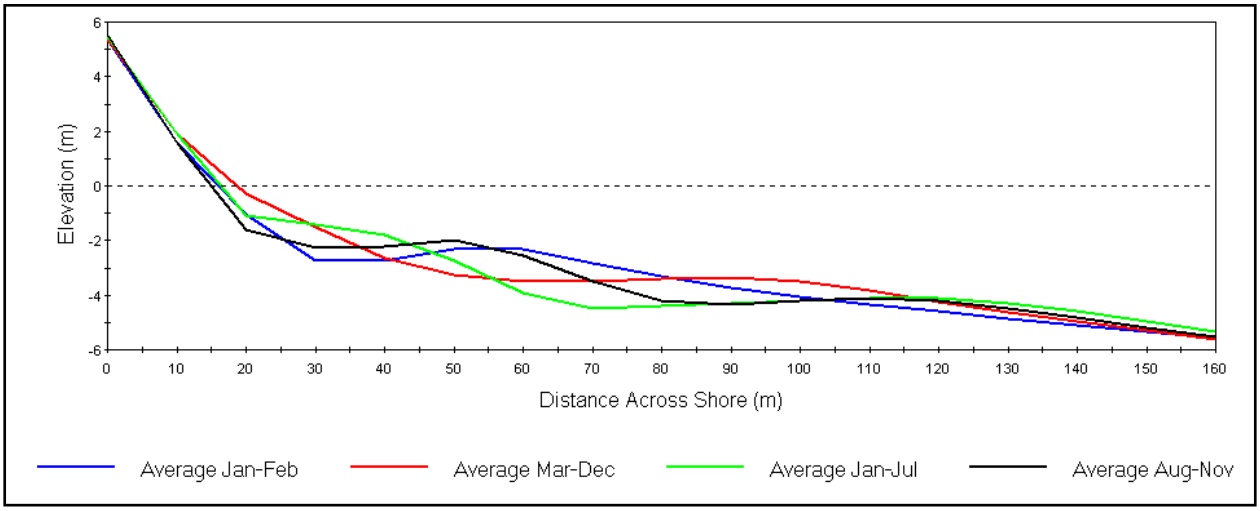

Figure 26. Average beach profiles for different periods with characteristic bar movement as deduced from the behavior of the principal scores.

SUMMARY: The Regional Morphology Analysis Package (RMAP) has been modified to add the capability of calculating Empirical Orthogonal Functions (EOFs) from beach profile and shoreline data with minimal input effort required from the user. EOF output may be generated quickly from any number of input profiles or shorelines. RMAP now provides the capability to visualize EOF modes along with profiles or shorelines within the same graphical user interface. EOF data may be exported from RMAP for external analysis, and report quality plots may be exported directly from RMAP. Although the EOF analysis method is a descriptive tool and leaves the analysis of the processes up to the interpreter, the input data determine the amount of variability in the EOF modes and the method can help the interpreter relate EOF signals to physical processes governing coastal change. This added RMAP capability presents engineers and scientists with additional tools to develop practical coastal data analysis applications.

PRODUCT DEVELOPMENT AND AVAILABILITY: RMAP, with the EOF routines, is available to both U.S. Army Corps of Engineers (USACE) and non-USACE interested parties. RMAP is available within the Coastal Engineering Design and Analysis System (CEDAS). For USACE employees, RMAP can be obtained by emailing to Alan Cialone in the Global Address Book. For non-Corps parties, please contact Veri-Tech at *sales@veritechinc.com*.

ADDITIONAL INFORMATION: This technical note was prepared by Kenneth J. Connell, research physical scientist, U.S. Army Engineer Research and Development Center, Coastal and Hydraulics Laboratory, and by Dr. Magnus Larson, Professor, Department of Water Resources Engineering, Lund University. The study was conducted as an activity of the Coastal

Morphology Modeling and Management (Cascade) work unit of the System-Wide Water Resources Program (SWWRP). For information on SWWRP, please consult *https://swwrp.usace.army.mil/* or contact the Program Manager, Dr. Steven L. Ashby, at *Steven.L.Ashby@erdc.usace.army.mil*. Questions about this technical note may be addressed to Kenneth Connell at (601-634-2840; *Kenneth.J.Connell@erdc.usace.army.mil*). This technical note should be cited as follows:

> Connell, K. J., and M. Larson. 2007. *Regional Morphology Analysis Package (RMAP): Empirical orthogonal function analysis, background and examples*. ERDC TN-SWWRP-07-9. Vicksburg, MS: U.S. Army Engineer Research and Development Center. *https://swwrp.usace.army.mil/*

REFERENCES

Aubrey, D. G. 1979. Seasonal patterns of onshore/offshore sediment movement. *Journal of Geophysical Research* 84(C10): 6347-6354.

Aubrey, D. G., D. L. Inman, and C. D. Winant. 1980. The statistical prediction of beach changes in southern California. *Journal of Geophysical Research* 85(C6): 3264-3276.

Batten, B. K., and N. C. Kraus. 2005. Regional Morphology Analysis Package (RMAP), Part 2: Users guide and tutorial. ERDC TN-SWWRP-05-1. Vicksburg, MS: U.S. Army Engineer Research and Development Center. *https://swwrp.usace.army.mil/*.

Davis, J. C. 1973. *Statistics and data analysis in geology*. New York: John Wiley & Sons.

De Vriend, H. J. 1991a. Mathematical modeling and large-scale coastal behaviour. Part 1: Physical processes. *Journal of Hydraulic Research* 29(6): 727-740.

De Vriend, H. J. 1991b. Mathematical modeling and large-scale coastal behaviour. Part 2: Predictive models. *Journal of Hydraulic Researc*h 29(6): 741-753.

Haxel, J. H., and R. A. Holman. 2004. The sediment response of a dissipative beach to variations in wave climate. *Marine Geology* 206: 73-99.

Hayden, B., W. Felder, J. Fisher, D. Resio, L. Vincent, and R. Dolan. 1975. *Systematic variations in inshore bathymetry*. Technical Report No. 10, Department of Environmental Sciences, University of Virginia, VA.

Horel, J. D. 1984. Complex principal component analysis: Theory and examples. *Journal of Climate and Applied Meteorology* 23: 1660-1673.

Hotelling, H. 1933. Analysis of a complex of statistical variables into principal components. *Journal of Educational Psychology* 24: 417-441; 498-520.

Hsu, T. W., S. R. Liaw, S. K. Wang, and S. H. Ou. 1986. Two-dimensional empirical eigenfunction model for the analysis and prediction of beach profile changes. *Proceedings of the 20th Coastal Engineering Conference* American Society of Civil Engineers, 1180-1195.

Hsu, T. W., S. H. Ou, and S. K. Wang. 1994. On the prediction of beach changes by a new 2-D empirical eigenfunction model. *Coastal Engineering* 23: 255-270.

Jackson, J. E. 1991. *A user's guide to principal components*. New York: John Wiley and Sons, Inc.

Kroon, A., M. Larson, I. Möller, H. Yokoki, G. Rozynski, J. Cox, and P. Larroude. In preparation. Statistical analysis of long-term morphological data sets from coastal areas. *Coastal Engineering*.

Krumbein, W. C., and F. A. Graybill. 1965. *An introduction to statistical methods in geology*. New York: McGraw-Hill.

Larson, M., and N. C. Kraus. 1994. Temporal and spatial scales of beach profile change, Duck, North Carolina. *Marine Geology* 117: 75-94.

Larson, M., and N. C. Kraus. 1995. Prediction of cross-shore sediment transport at different spatial and temporal scales. *Marine Geology* 126: 111-127.

Larson, M., H. Hanson, N. C. Kraus, and J. Newe. 1999. Short- and long-term responses of beach fills determined by EOF analysis. *Journal of Waterways, Port, Coastal, and Ocean Engineering* 285-293.

Larson, M., M. Capobianco, H. Jansen, G. Rozynski, H. Southgate, M. Stive, K. M. Wijnberg, and S. Hulscher. 2003. Analysis and modeling of field data on coastal morphological evolution over yearly and decadal time scales. Part I: Background and linear techniques. *Journal of Coastal Research* 19(4): 760-775.

Liang, G. L., and R. J. Seymour. 1991. Complex principal component analysis of wave-like sand motions. *Proceedings of Coastal Sediments '91*, ASCE: 2175-2186.

Liang, G., T. E. White, and R. J. Seymour. 1992. Complex principal component analysis of seasonal variation in nearshore bathymetry. *Proceedings of the 23rd Coastal Engineering Conference.* ASCE: 2242-2250.

Medina, R., C. Vidal, M. A. Losada, and A. J. Roldan. 1992. Three-mode principal component analysis of bathymetric data, applied to 'Playa de Castilla' (Huelva, Spain). *Proceedings of the 23rd Coastal Engineering Conference*, ASCE: 2265-2278.

Preisendorfer, R. W. 1988. Principal component analysis in meteorology and oceanography. *Developments in atmospheric sciences.* 17. Amsterdam, The Netherlands: Elsevier.

Rozynski, G. 2003. Data-driven modeling of multiple longshore bars and their interactions. *Coastal Engineering* 48: 151-170.

Ruessink, B. G., I. M. J. Van Enckevort, and Y. Kuriyama. 2004. Non-linear principal component analysis of nearshore bathymetry. *Marine Geology* 203: 185-197.

Stauble, D. K., A. W. Garcia, N. C. Kraus, W. G. Grosskopf, and G. P. Bass. 1993. *Beach nourishment project response and design evaluation: Ocean City, Maryland. Report I. 1988-1992*. Technical Report CERC-93-13, Vicksburg, MS: U.S. Army Engineer Waterways Experiment Station.

Stauble, D. K., and G. P. Bass. 1999. Sediment dynamics and profile interactions of a beach nourishment project. *Proceedingsof Coastal Sediments 99.* ASCE: 2,566-2,581.

Von Storch, H., and A. Navarra. 1995. Analysis of climate variability. *Applications of statistical techniques*. Berlin, Germany: Springer Verlag.

Weare, B. C., and J. S. Nasstrom. 1982. Examples of extended empirical orthogonal function analysis. *Monthly Weather Review* 110: 481-485.

Wijnberg, K. M. 1995. *Morphologic behavior of a barred coast over a period of decades*. Unpublished Ph.D. dissertation, Utrecht, The Netherlands: University of Utrecht.

Wijnberg, K. M., and J. H. J. Terwindt. 1995. Extracting decadal morphological behaviour from high-resolution, long-term bathymetric surveys along the Holland coast using eigenfunction analysis. *Marine Geology* 126: 301-330.

Winant, C. D., D. L. Inman, and C. E. Nordstrom. 1975. Description of seasonal beach changes using empirical eigenfunctions. *Journal of Geophysical Research* 80(15): 1979-1986.

Yokoki, H., and M. Larson. 2004. Complex principal component analysis to characterize beach topographic change in Sylt Island, Germany. *Proceedings of the 2nd International Conference on Asia and Pacific Coasts* (CD-ROM).